THE EFESTO PROJECT: FLEXIBLE TPS DESIGN AND TESTING FOR ADVANCED EUROPEAN RE-ENTRY SYSTEM BASED ON INFLATABLE HEAT SHIELDS

Thorn Schleutker[1], Burkard Esser[1], Ali Guelhan[1], Jean-Luc Verant[2], Nicolas Dellinger[2], Yann Dauvois[2], Giovanni Gambacciani[3], Giuseppe Guidotti[4], Giuseppe Governale[5]

[1] DLR, Deutsches Zentrum für Luft- Und Raumfahrt e.V., Köln, Germany
[2] ONERA, Office National d'Etudes et de Recherches Aerospatiales, Toulouse, France
[3] AVIOSPACE srl, Turin, Italy
[4] DEIMOS Space S.L.U., Tres Cantos 28760, Spain
[5] Department of Mechanical and Aerospace Engineering, Politecnico di Torino, Turin 10129, Italy

ABSTRACT

The European Union H2020 project EFESTO has been implemented with the main objective to improve the technology readiness level (TRL) of flexible inflatable heat shields for re-entry vehicles in Europe from 3 to 4 or 5. For this purpose, two reference missions with atmospheric entry to Earth and Mars were selected. Both missions were designed to make best use of the Hypersonic Inflatable Aerodynamic Decelerator (HIAD) concept. Multidisciplinary design loops allowed prediction of the entry flight trajectory and identification of the aerothermodynamic environment on the exterior of the system. These results were the primary inputs to the design and testing of the Flexible Thermal Protection System (FTPS) layup and the underlying inflatable structure.

This paper provides an insight into the efforts related to design, testing and numerical modelling of the FTPS for both applications. Advanced flexible materials were selected, some of which never had been considered in Europe before. These materials allow for a significant improvement upon previous design in system weight and maximum heat loads. Several multi-layer layups were developed for both applications, each of them allowing to keep the surface temperature below the material-specific upper limit. The most promising layups were selected for experimental simulation in DLR's arc-heated facilities LBK at flight relevant high-enthalpy conditions in realistic thermochemical environment. This testing covered both stagnation flow and tangential flow conditions in Mars and Earth atmospheres. Extensive numerical efforts were carried out to perform test rebuilding and allow cross-correlation between numerical and experimental simulations. The numerical models were calibrated with the wind tunnel data and further assisted in the analysis of the experimental results and the derivation of material specific properties and uncertainties.

The project allowed to validate numerical models and simulations tools. This enables Europe to reliably design FTPS layups in future initiatives in the strategic field of re-entry solutions based on inflatable heat shields.
This project has received funding from the European Union's Horizon 2020 research and innovation program under grant agreement No 821801.

Keywords: Inflatable Heat Shields, Flexible TPS, Aerothermodynamics, Arcjet Testing, Inflatable Structure, Aerodynamic Decelerators.

1. INTRODUCTION

EFESTO targets the definition of critical space mission scenarios in Earth and Mars applications that are enabled by the use of advanced inflatable Thermal Protection Systems (TPS). This includes the characterization of the operative environment and the validation of the developed Flexible TPS (FTPS) by tests of both the flexible layups used for thermal protection and the inflatable structure beneath. The thermal validation of the layups is done via simulation in high-enthalpy wind tunnel facilities using Earth and Mars atmosphere. The inflator is tested separately and at a 1:1 scale for exploration the morphing dynamics and materials response when being inflated from a packed to the fully inflated configuration. The results of all tests assist the consolidated design of a future in-orbit demonstrator mission.

The flexible TPS is one of the key technologies for enabling inflatable heat shields and to bring them closer to operational applicability in development of re-entry capsules and aero-braking systems used for safe atmospheric re-entry. The highest TRL thus far has been achieved by NASA. They have developed this technology via different initiatives, ranging from theoretical development and ground testing to flight verification ([1] to [6]).

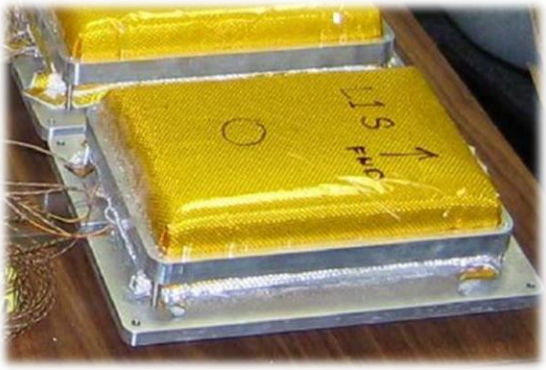

Figure 1: NASA FTPS sample before testing [3].

The European Space Agency and the European Commission have recently fostered the development of FTPS technologies to improve their TRL in Europe. This includes different initiatives with EFESTO being one of them ([7] to [9]). The EFESTO project contributes to increasing the TRL in several ways. The work conducted on the design and testing of the flexible TPS is presented in this paper.

2. FTPS DESIGN

The mission and system design definition executed by the EFESTO team during the first part of the project allowed to have a set of requirements for the specific design of the flexible TPS layup. The work started with definition of possible stacked configurations of different available materials, such as woven and non-woven, fabrics and blankets etc. The materials were selected based on their thermal characteristics as stated in their datasheet and the results of the experimental material characterization.

The methodology for thermal modelling and analysis was based on identifying the most critical areas to which the FTPS shall be applied and to adopt a one-dimensional modelling to the different multi-layer configurations with the specific material definition of each of the layers.

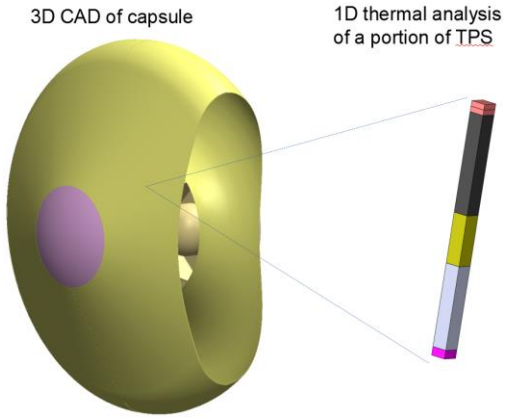

Figure 2: FTPS numerical modelling approach.

This modeling allowed to build different configurations by varying the material layers in terms of their thickness and thermal characteristics. All materials identified to be interesting were rated based on former application in other space programs, availability in Europe, native size of blankets or rolls, resistance to oxidation, mechanical characteristics (behavior of the material under tensile load or compression), density, ability endure sharp bends, handling and stability over time. The configurations were defined considering the capsule geometry and the mission environment.

The thermal shield was divided into different areas based on the location on the inflator and the experienced local thermal loads with the aim to optimize the TPS configuration and relative mass of each area (nose, windward, edge and back-shield). As the idea is to use a rigid TPS on the nose, the windward area requires the thickest and most complex flexible TPS layup.
The analyses provide predictions for the temperature development over the entry flight time. In an iterative cycle, the design of the layup was adjusted regarding the thermal results of the previous runs and the material capabilities and a set of promising configurations was finally defined for experimental entry flight simulations.

3. MATERIAL CHARACTERIZATION

Knowledge of the material specific thermophysical properties is required for the TPS design and the numerical simulations. Accordingly, the relevant thermophysical properties of all materials used for the flexible TPS layups where characterized in the EFESTO project. The work was conducted in the laboratory of the Austrian Foundry Institute ÖGI. The targeted properties are the specific heat, thermal conductivity and diffusivity and the mass loss. The properties are temperature dependent, so they were measured in a broad temperature range. The lower temperature limit of the range was the room temperature (except for specific heat measurements, which started at 100°C). The upper temperature limit was 1100-1300°C, depending on the material and the applied technique. Pyrogel XTE is stated by the manufacturer to be usable at up to 650°C. The thermal limit of the aerogel based super insulation was generally regarded except for the mass loss investigation, where all materials were tested up to 1300°C. Where necessary, the properties were extrapolated to temperatures below or above the measured range based on behavior described in the literature.

Some of the measurement techniques require knowledge of the test specimen thickness – which was found to be a problem. The flexible materials do not provide a sound surface for thickness measurement or definition. The flexible cloths are uneven because of their woven nature and the fiber felts are not only quite compressible, but also have no defined surface. The fine fibers of the felts tend to fray, which means that there is a smooth transition between the material and the void surrounding. The thicknesses were measured several times and averaged.

The areal weight and the density at room temperatures were calculated from the sample weight and dimensions. The materials all showed some deviation (up to 7%) from the manufacturer data.

The specific heat capacity was measured via differential scanning calorimetry with a heating rate of 20 K/min. The mass loss was measured with simultaneous thermogravimetry at a heating rate of 5 K/min. The thermal diffusivity was measured via the laser flash method in steps of 100K. These three techniques all used a protective pure argon atmosphere. The thermal conductivity was calculated from the density, thermal diffusivity and specific heat.

The correlation between compression of the material and its thermal conductivity was investigated at room temperature using the thermal hot bridge technique. The material stacks were compressed by a specific pressure and the remaining thickness was compared to the nominal value to calculate the percentage of compression. The thermal conductivity showed the expected clear correlation to the compression except for the aerogel material. The thermal conductivity of Pyrogel XTE did not change significantly when compressed.

Additional to the thermophysical characterization of the materials, ÖGI performed also thermal simulations of the complete FTPS layup with a novel approach: instead of heating the flexible TPS layup with an external heat source at a constant heat flux, the external surface of the cold test sample was exposed to a high constant temperature. The exposure to the high temperature was realized by setting a graphite crucible filled with liquid copper on top of the layup. The graphite's high thermal conductivity ensure that the top fabric reaches the nominal melting temperature of the copper very quickly. The slow freezing of the pure copper, that happens at a constant temperature, ensures that the temperature experienced by the top fabric remains stable over a long duration of time.

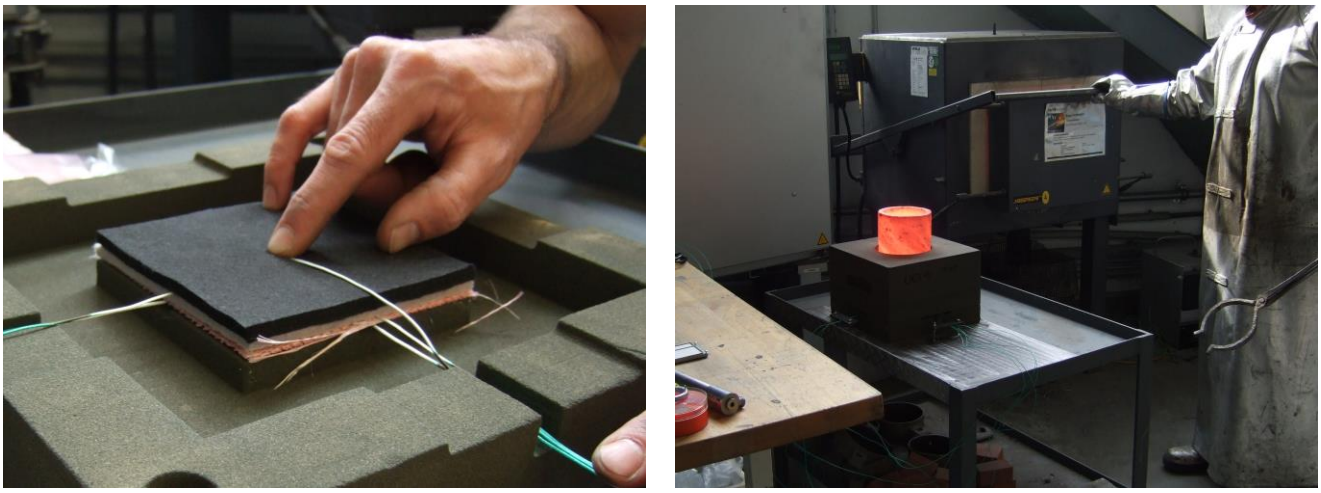

Figure 3: FTPS sample being integrated (left) and the finished sample during the thermal test (right).

The samples were embedded in a form created from casting sand by additive manufacturing. The square sample were smaller than the round crucible, so that the full surface of the test sample was exposed to the high temperature and the crucible at the same time stood on the rigid sand form. The latter allowed to design a specific compression of the layup into the sand form. This was of special interest as a defined compression of the flexible layup is not possible in the wind tunnel testing. Also, these thermal tests provide excellent data for calibration of the numerical simulation because of the well-defined boundary conditions.

Figure 3 shows the test sample while being built and during the actual thermal test. The thermocouple integration of these thermal tests was the same as that being used for the wind tunnel experiments, which is described in the next section.

4. EXPERIMENTAL SIMULATIONS

The experimental entry flight simulations were performed in the arc heated wind tunnel facilities LBK of DLR in Cologne. The purpose of these simulations is the characterization of the thermal performance of the developed FTPS layups and its ability to survive the thermally and chemically aggressive entry flight environment.

Wind tunnel facilities

The LBK facilities consist of the two legs L2K and L3K, which share the vacuum pump and exhaust gas cleaning system.

The L2K wind tunnel uses a Huels-type arc heater with a maximum electrical power of 1.4 MW to heat the test gas to high enthalpy conditions. This heater allows cold wall heat fluxes up to 3.0 MW/m² at stagnation point pressures up to 250 hPa, depending on the selected nozzle, sample dimensions etc. The flow is accelerated to hypersonic conditions in the conical convergent-divergent nozzle with a half angle of 12°. Throat diameters of 14 mm, 20 mm, 25 mm and 29 mm are available and can be combined with nozzle exit diameters of 50 mm, 100 mm and 200 mm. This allows adapting the L2K to particular necessities of a certain test campaign in a very broad range. Additionally, the arc heater allows very flexible selection of the test gas. Gases and mixtures such as Air, Nitrogen, Argon, Carbon Dioxide or Martian atmosphere have been used in the past.

The L3K uses a more powerful segmented type arc heater that can be operated with an electrical power of up to 6 MW. This allows the wind tunnel to achieve cold wall heat fluxes beyond 10 MW/m² at stagnation point pressures up to 2000 hPa. However, the arc heater is less flexible and the only test gas option is air with a small Argon addition. The L3K uses a very similar conical nozzle geometry as the L2K. The half angle, throat and exit diameters are the same. The higher mass flow rates and gas pressures possible in this wind tunnel allow wider nozzle exit diameters and a nozzle with a 300 mm exit is available.

Figure 4 shows a schematic of facilities. A more detailed description of the facility is given by Esser [10] and Gülhan [11].

In the EFESTO project, both the L2K and L3K were used and set up with a 29 mm nozzle throat and 100 mm and 200 mm wide nozzles. The L2K was operated with air for simulation of the entry flight in the atmosphere of earth. For the simulation of entry into the atmosphere of mars a mixture of Carbon Dioxide and Nitrogen (3% by mass) was used.

Test setups

Two different setups were used for the simulations: the stagnation setup and the tangential setup. The stagnation setup allows experiments with high heat flux levels. Because of the stagnation flow, aerodynamic forces acting on the test sample are rather small and the setup allows investigation of the behavior with only the chemical and thermal boundary conditions being represented. The tangential setup focuses on the influence of a tangential flow and the shear forces created by the surface parallel flow component. However, the tangential setup is rather limited in the achievable heat fluxes, so compromises had to be made.

The stagnation setup assembly's geometry is a flat-faced cylinder with a diameter of 70 mm and an edge radius of 11.5 mm. The configuration is well-suited for stagnation tests as it generates a nearly uniform heat flux distribution on the flat front surface.

The external shape at the edge and on the side is formed by a graphite shell. On the front, the shell has a circular opening with a diameter of 45 mm. This area is covered by the external

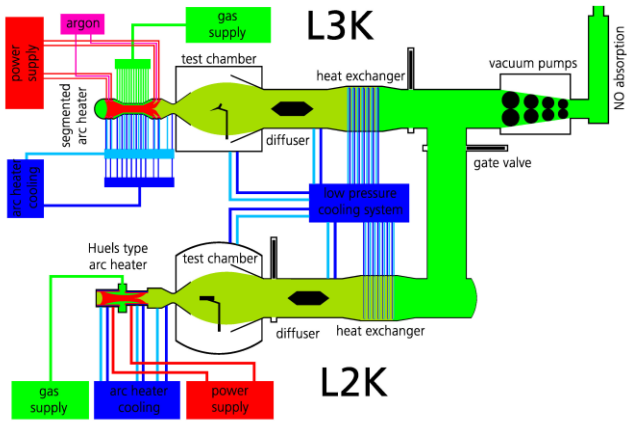

Figure 4: LBK facility sketch.

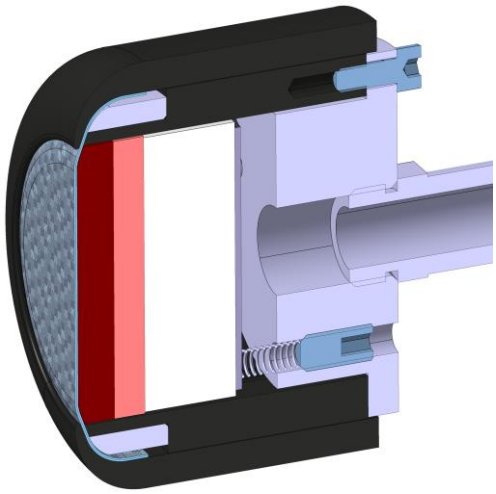

Figure 5: Cut of the stagnation setup CAD.

fabric layers of the flexible TPS layup. The specimens of the outer fabric are circular with a diameter of 70 mm. They extend around the rounded edge to the side and are held in position by the clamping jacket, that is also made of graphite and fits into the shell's internal diameter. Together with an adaptive collar on its top, the jacket is pressed against the front of the shell, thus fixing the fabric layers.
The insulation layers and closing fabrics are integrated from the rear end into the interior of the clamping jacket. They are prepared as circular specimens with a diameter of 46 mm and placed layer-by-layer.
A rigid insulator is installed at the bottom end to isolate the test sample from the support plate. The 1mm thin stainless-steel plate provides a rigid interface and keeps the layup in place. The backing plate is held by three spring supported pins. Adjustment screws in the end cover allow for setting a compression force to the backing plate in order to achieve a realistic mechanical environment similar to the compression during flight after inflation of the TPS and preventing void in the TPS layup.

The tangential setup produces a tangential flow that creates shear stress on the front surface the FTPS specimen. The tangential flow is realized by integrating the test sample into the integration bay of a flat plate model holder such that the test articles surface is flush with the top plate of the holder.
In the tangential setup, the sample is built around the central part: the square graphite jacket. The external fabric layers of the sample layups are placed on top of the jacket. Lateral extensions in the fabric layer are bent around the jacket and fixed with clamping mechanisms at each side. The jacket with has an inner cross-sectional area of 80 x 80 mm². The interior volume is filled with the insulation layers and the bottom fabrics of the FTPS layup. The layers are integrated layer-by-layer from the back. The specimens are quadratic with an

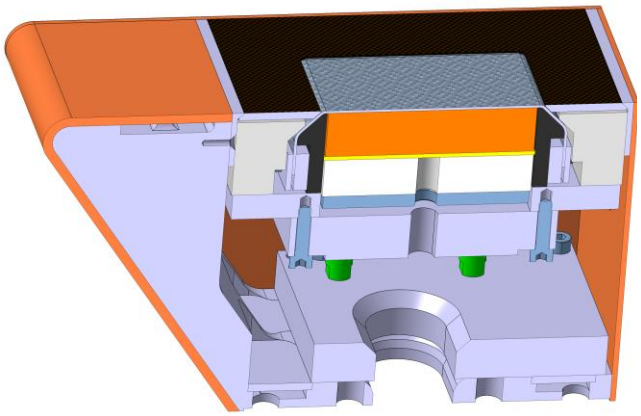

Figure 6: Cut of the tangential setup CAD.

edge length of 80 mm. A rigid insulator is installed at the bottom end as additional insulation and the layup is closed with a metallic backing plate. The jacket is then mounted on a support plate.
Similar to the stagnation setup, adjustment screws in the tangential setup allow setting a defined compression force via a spring loading mechanism.
The assembly is surrounded by rigid insulation to avoid parasitic thermal loading from the sides. The top surface is closed by a ceramic cover plate. The cover plate leaves an open area of 80x80 mm² for the flexible TPS layup sample.

Testing overview

The experimental entry flight simulations were conducted in three different wind tunnel test campaigns. The first campaign targeted the thermal behavior and survivability of the flexible TPS layups using the stagnation setup. In this campaign, a total of 26 tests was conducted on the one Earth and the two Mars layups in the L2K facility. The test samples were exposed to different heat flux levels and total heat loads in air and Mars gas mixture. The test samples endured plasma flows with up to 780 kW/m² of measured cold wall heat flux and up to three minutes of test duration.

Figure 7: Stagnation (left) and tangential (right) setups during experimental entry flight simulations.

In the second test campaign 21 tests were performed using the tangential setup in L2K and L3K. The larger L3K facility was necessary to produce representative heat loads. However, even with this more powerful facility, the most extreme test condition generated a cold wall heat flux of only 380 kW/m². The campaign aimed at the influence of the tangential nature of the flow on the FPTS. A potential failure of the external fabrics due to the combined thermal and mechanical load was to be ruled out. Different heat flux levels and test durations were combined.

The last test campaign used the stagnation setup and focused on investigation of details that had not been addressed in the previous campaigns. This included testing of the repeatability, the addition of the rear layers of the FTPS to the stack (the Zylon fabric and the Kapton gas barrier) and the performance of the FTPS design in the shoulder and aft region of the inflatable decelerator. The shoulder region is characterized by lower heat loads and a step-wise reduction of the number of insulative layers and tested by varying the heat load and the number of insulation layers. This campaign consisted of a total of 20 tests; ten tests on the earth layup A1 and its variations and the same number of tests on the Mars layup M6 and its variations. The investigation of the second mars layup D5 was discontinued as it was regarded inferior to M6.

The ability of the FTPS layups to survive the aggressive thermal and chemical entry flight environment was proven by the footage of the experimental simulations captured in the visual range with HD cameras and via post-test investigation of the specimens.
The other major goal, the characterization of the thermal performance and the providing of reference data for numerical rebuilding both demanded the measurement of the temperature distribution and development during the test. Accordingly, several different techniques were applied for this purpose.
The temperature of the exposed surface of the outer fabric was measured remotely. A set of two pyrometers, a spectral pyrometer and a two-color pyrometer, measured the temperature of the center of the sample in the narrow wavelength range (0.85-1.1 µm). The temperature distribution on the surface was gathered by different infrared cameras. However, the results of these remote techniques depend on the emissivity of the surface. The emissivity changes with temperature, chemical composition of the surrounding gas, duration of the exposure, thermal gradient inside the top fabric and other parameters. Therefore, the data of the remote instruments has a high uncertainty and is not suited as reference data for the numerical rebuilding.
Therefore, the internal temperatures were also addressed. They were measured with thermocouples integrated in between the different layers and at the center of the of the FTPS samples. The thermocouple data is ideal for comparison of test and numerical rebuilding results.

Experimental results

The hot phase of an atmospheric entry flight typically takes only a few minutes. Accordingly, the continuous use temperature of the materials provided by the manufacturers can be a quite conservative threshold in the design of the heat shield. If the materials can stand higher temperatures, design that result in higher heat loads and material temperatures become possible. This is highly desirable. Steeper entry flight trajectories, for example, increase the peak heat flux value and the temperatures experienced at and near the surface, but they reduce the duration of the hot phase and integral heat load and thus also the amount of insulation required. Therefore, materials with higher use temperatures allow for more efficient FTPS designs.
On the other hand, the materials are exposed to conditions that are not only extreme regarding the temperatures. The materials might well fail because of the chemically aggressive environment: the extreme heating of the gas over the bow shock and the subsequent thermal decomposition produce highly reactive species, such as atomic oxygen. These species can react with the outer FTPS materials and might burn them at temperatures below their nominal continuous use temperature.
It is thus of utmost interest to reveal the true potential of the materials for the FTPS application with its short exposure timeframe and aggressive environment. This has been addressed by exposing the samples to different heat flux levels and heat loads.

The Hi-Nicalon Type S used as the outer fabric survived all heat fluxes and heat loads both in air and Martian atmosphere mixture without failing. The only sign of the exposure was the discoloration and a stiffening of the fabric. Both effects were likely caused by a limited oxidation of the silicon carbide with formation of a silicon dioxide layer on the fibers. Figure 8 shows an outer fabric specimen before and after a test at the highest heat flux condition. The test sample has experience more than 1500°C for one and a half minutes.

Sigratherm KFA and Sigratherm GFA are both felts made from fibers that are composed mainly of carbon with the GFA having a smaller ash content. However, apart from this difference, the thermal properties of the two high-temperature insulation materials are very similar. Accordingly, they also behaved very similar in the wind tunnel test. Both materials were able to withstand temperatures of 1500°C, but both materials also lost a relevant amount of mass due oxidation. This exemplarily shows that the materials can be suited for

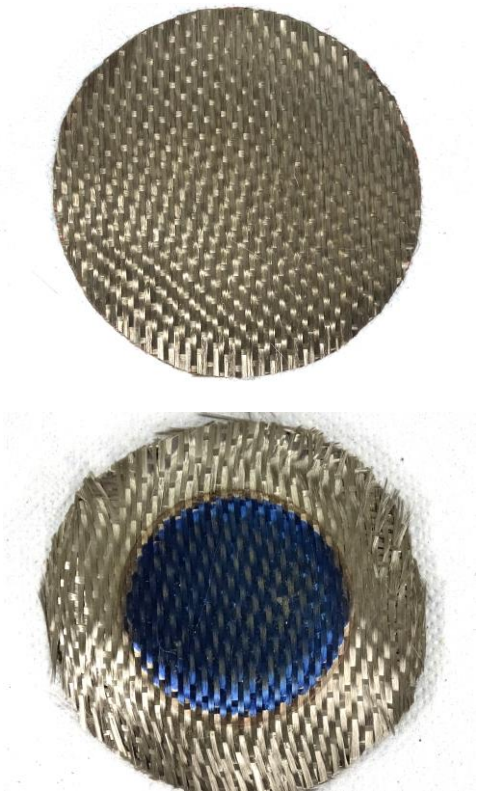

Figure 8: Hi-Nicalon Type S fabric before (top) and after (bottom) the wind tunnel test.

higher conditions for the short time of the hot entry flight phase.
Sigratherm GFA showed shrinkage and cracking at the most extreme temperatures, while the KFA remained intact at the same condition. Additionally, a thick version of GFA had been used. The single 15mm layer showed less flexibility for reduction of the insulation in the shoulder area of the inflator. Therefore, the last test campaign omitted the GFA and concentrated on KFA instead.

The aerogel-based Pyrogel XTE was a negative surprise. The material does have an outstanding insulation performance and would allow reduction of the thickness of the insulation, but the continuous use temperature stated by the manufacturer really is the limit of the material. At temperatures above 700°C, the material shrinks and forms cracks. While the material did not fail completely in any of the tests, the hotter side was also always degraded. Figure 9 shows an example with strong degradation.
Additionally, the material is rather stiff and tends to crack when bent. These are quite bad properties for a flexible TPS that is to be stowed in a small volume before inflation. The material also loses a lot of dust when handled, which may become an issue for integration into a spacecraft. And finally,

Figure 9: Pyrogel XTE after exposure to 1000°C.

the material is very inhomogeneous. The density and thickness of Pyrogel XTE vary not only between different batches of the material but also on small scales. Accordingly, the repeatability of the thermocouple data in test with Pyrogel was poor. This could become an issue in the FTPS design and qualification.

The Nextel 440 used as rear fabric was obviously not harmed by the heat. The material did not experience temperatures anywhere near its thermal capabilities. Accordingly, the Nextel layers only reacted to the test with a change of color that was caused by the thermal removal of a part of the seizing.

The Zylon and Kapton were heated to temperatures slightly above 400°C in some tests. The Zylon is rated for up to 650°C, so this material obviously had no problem with the experienced conditions.
The Kapton, also did not show any optical sign of failure or thermal decompositions. This does not necessarily mean that the material would still have been gas-tight and it might suffer from aging and radiation embrittlement before the entry flight in the application field. Therefore, a conclusion on the thermal capabilities of Kapton in short term exposure cannot be based on the visual test results.

5. NUMERICAL SIMULATION

The purpose of the numerical modelling is the validation and improvement of aero-thermodynamic and thermal models using CFD Navier-Stokes and material response solvers. This is achieved by comparison of the numerical results against the test data collected by DLR during the experimental ground tests in their high-enthalpy wind tunnel facilities. The numerical methodology should confirm the relevance of the chosen numerical/physical approach in the solvers. The numerical tools will also be used for assessment of the catalytic recombination parameters associated to the Hi-

Nicalon. The understanding of the catalytic interaction of the outer fabric with the incoming flow in both Earth and Mars atmosphere is important for the heating safety margin to be applied in ground-to-flight extrapolation.

Numerical rebuilding methodology

The rebuilding of the wind tunnel tests is based on coupling the CFD platform CEDRE [12], in particular its fluid solver CHARME, and the material response code MoDeTheC [13], both developed at ONERA. The coupling is achieved through the CWIPI library, also developed at ONERA. The numerical rebuilding methodology is divided into four sequential computational steps.

The first step in the numerical rebuilding is the determination of the reservoir gas composition. The mass flow rate and the reservoir pressure of the gas are measured and controlled during the experimental simulation. These parameters are used to initiate the calculation of the total enthalpy and the reservoir temperature via the conservation of mass and energy. An isentropic flow in thermochemical equilibrium state is assumed between reservoir and nozzle throat. The pressure and temperature inside the gas-filled reservoir in combination with the assumed thermo-chemical equilibrium allow determination of the chemical composition of the gas. In EFESTO, the 5-species (N_2, O_2, N, O, NO) thermochemical kinetic model of Park for Earth's atmosphere [14] and the 10-species thermochemical kinetic model (CO_2, CO, C, C_2, CN, O_2, O, N_2, N, NO) of Park for Martian atmosphere [15] are used.

The subsequent step is the simulation of the flow through the nozzle and the test chamber with the CFD solver CEDRE. The flow is simulated two-dimensional and axisymmetric assuming chemical non-equilibrium from the nozzles throat downwards. The Navier-Stokes solver CHARME is used for stagnation and tangential setups and Earth and Mars atmospheres. The nozzle and the test setup geometry were first reproduced according to the provided design data. The boundary conditions were set to those used in previous projects [16]. The inlet is fully characterized by the total pressure, the total temperature and the gas composition that were derived in the previous step. The nozzle walls are considered super-catalytic at a temperature of 500 K. Chemical equilibrium (79% N_2, 21% O_2 for Earth and 97% CO_2, 3% N_2 for Mars) is assumed at this boundary. A large test chamber is modelled to prevent the interaction of nozzle reflected acoustic waves with the model. The test chamber background is numerically modelled as low-pressure and cold air (20 Pa at 300 K) at chemical equilibrium (79% N_2, 21% O_2). The wall of the test chamber around the nozzle exit is considered non-catalytic with a temperature of 300 K. Preliminary computations showed that different catalytic wall assumptions applied on different surfaces did not affect the expanded flow resulting from the simulation. Preliminary computations of the flow rebuilding around metallic catalytic probes designed were used to assess the capability of the CFD models in rebuilding measured heat flux rates. The margins of such rebuilding are in the range of 15% to 40%, depending on the setup and the atmosphere.

Next, the optical and chemical wall properties of the samples can be determined with the inverse method. The emissivity of the Hi-Nicalon outer fabric was not characterized. Therefore, the emissivity of this silicon carbide fiber was derived by assuming radiative equilibrium on the material samples and using literature values for the catalytic recombination parameters of solid silicon carbide [17]. The equilibrium temperature at the center of the sample was compared to the experimental measurements to adjust the emissivity. This assumption is justified because of the low thermal conductivity of the Hi-Nicalon fabric, which gives a low contribution of conductive heat transfer inside the material to the thermal balance at the surface of the sample compared to convective and radiative cooling mechanisms.
The heat flux on the Hi-Nicalon surface was estimated using the inverse method implemented in ONERAs thermal solver THIDES [18]. Knowing the thermo-physical properties of the materials and the temperature below the Hi-Nicalon during the test, the heat flux density through the outer fabric and the surface temperature were calculated for each layup, setup and gas atmosphere. The boundary of the innermost layer of the FTPS was assumed adiabatic. Also, ideal thermal contacts were assumed between each layer of the layup.
Rough values of the catalytic recombination parameters were finally estimated for each atmosphere and test setup. This was achieved by an iterative process in which the catalytic efficiency in the numerical model was adjusted and the resulting heat flux prediction was compared to the one obtained by the inverse method with an identical constant surface temperature. Changing the emissivity was necessary for the tangential setup tests to maintain the values of the catalytic recombination parameters within reasonable ranges.

Finally, numerical rebuilding of the layups allowed comparison against the temperature profiles measured within the samples. For this purpose, the CFD simulations were coupled with the material response code MoDeTheC. At the fluid/solid interface, the heat flux predicted by CHARME and radiative cooling are accounted. Below the rigid insulator and on sides of the sample, adiabatic conditions were assumed. The predicted surface temperature was fed back into the CFD simulation.
For the stagnation setup, the temperature of the holder was fixed to 300 K with identical catalytic recombination parameters as the sample. This exact boundary parameters are

non-relevant in this case as the flow along the shoulder and side of the holder does not have an influence on the sample in the supersonic flow. However, for the tangential setup, the flow along the holder that is upstream the sample has an influence on the heat flux distribution on the sample. This is pronounced by the catalytic recombination mechanism of oxygen and nitrogen. Therefore, the holder temperature was set to 500 K as this number was estimated as realistic temperature and the surface of the holder was considered fully catalytic.

The coupling between the fluid and the solid domains is quasi-steady, which means that the CFD simulations are converged at each coupling step with the material solver. This allows following the dynamic heating phase of the test sample in spite of the very different time scales of the physical phenomena in each computational domain. The chosen coupling time step was verified to have no major influence on the material response.

Results of the wind tunnel rebuilding

Two exemplary results of the numerical modelling of the wind tunnel flow are illustrated in Figure 10. The left image shows the Mars atmosphere flow in the L2K with the stagnation setup in its test position. The right image in
Figure 10 shows the Earth atmosphere flow of L3K with the tangential setup.

Once the first flow solution is established the iterative coupling process between the CFD solver and the thermal solver is realized to determine the thermal response of the exposed test sample.

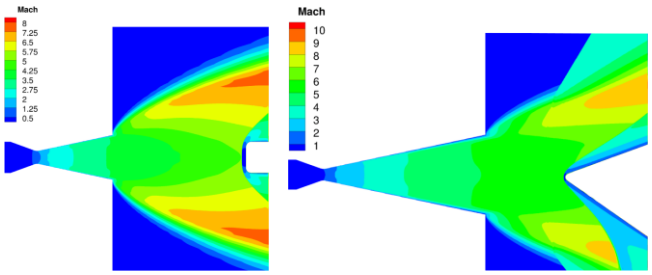

Figure 10: Results of the numerical rebuilding of the wind tunnel flow. The stagnation setup in Mars atmosphere in L2K is left, the tangential setup in Air in L3K is on the right.

Results of the thermal response simulations

Figure 11 shows two graphs that compare the measured temperature trends (dashed lines) against the results of the numerical rebuilding (solid lines). For this comparison, test cases with the stagnation setup being exposed to the highest heat flux in Earth atmosphere and to the lowest one in Mars atmosphere were chosen. The graphs show a good agreement between numerical rebuilding and measurements. The surface temperature profiles show that the surface properties, i.e. emissivity and catalytic efficiency of Hi-Nicalon, are consistent. The temperatures measured by the thermocouples at the interfaces of different material layers are generally rebuilt well. Though, it remains unclear whether the discrepancy is caused by the thermal inertia of the thermocouples in their highly insulative environment or by deficiencies in the numerical rebuilding. A problem was that in the given tests the sample was moved into the test position within roughly two seconds. In this period the sample passes through the flow and is heated before the nominal start of the test. The numerical rebuilding assumes the cold sample to be exposed to the hot flow immediately. This was addressed in the last test campaign by using a pneumatic shield for quick exposure of the sample.

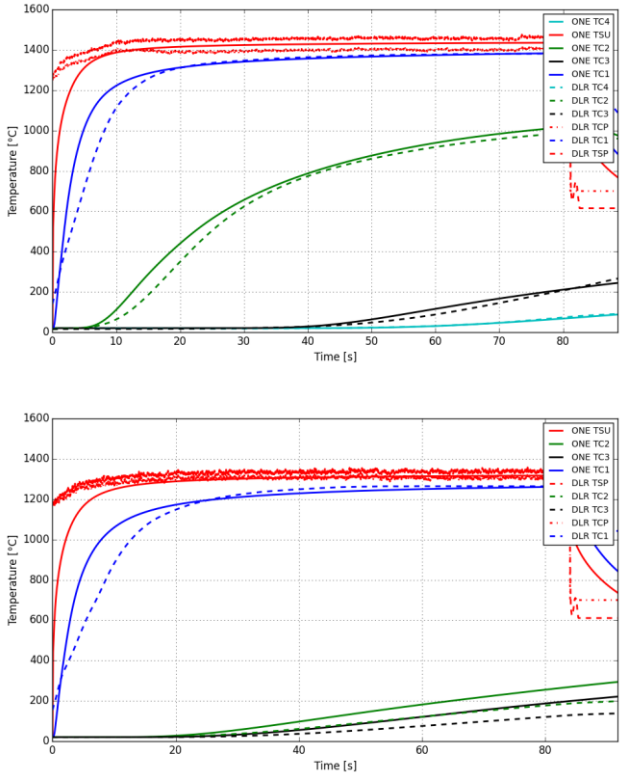

Figure 11: Temperature profiles of the stagnation configuration in Earth atmosphere at the highest heat flux (top) and in Mars atmosphere at the lowest heat flux (bottom).

Figure 12 shows the same comparison for the tangential setup. Again, the Earth and Mars atmosphere tests where the samples were exposed to the highest heat flux were taken. The limitation of the tangential setup regarding the achievable heat flux becomes apparent when considering the

lower surface temperatures. As for the stagnation setup, the numerical rebuilding is in good agreement with the measurements but the heating dynamics is not perfectly captured.

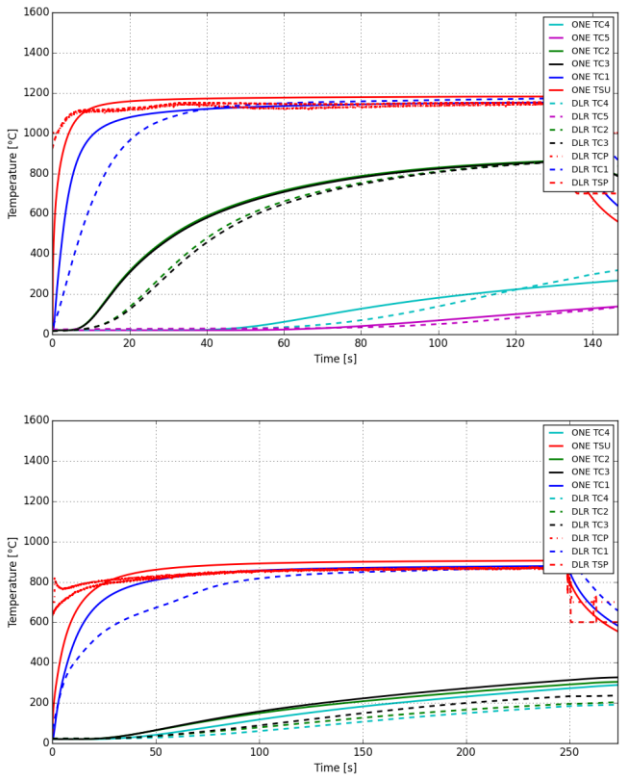

Figure 12: Temperature profiles of the tangential configuration in Earth (top) and Mars (bottom) atmospheres at the highest respective heat flux.

6. CONCLUSIONS

This paper briefly describes the work in the design, evaluation and modelling of the flexible thermal protection systems for the two reference missions of the EFESTO project. The vast extend of work does not allow a full representation within a single conference paper. Accordingly, this document only gives an overview of the conducted work and some representative examples and most interesting findings. For further information, please refer to the official EFESTO documentation and the companion papers at this conference.

The validity of the design of the different flexible heat shield layups developed early in the project was proven via experimental simulations. These tests also revealed that several of the chosen materials have the capability to survive temperatures far beyond their continuous use temperature. This allows for further improvement of the designs in the near future.

The experimental data has also been used for validation and calibration of the numerical tools. Accordingly, these tools can now be used for further development of the FTPS designs and reference mission definition.

The concept of a flexible TPS that protects an inflator from the harsh entry flight environment was shown to be feasible. Therefore, the authors believe that the concept is worth pursuing and should be brought to a higher TRL in a subsequent project. The path towards an in-flight demonstrator and actual application of the technology is now clear.

7. ACKNOWLEDGMENTS

This project has received funding from the European Union's Horizon 2020 research and innovation programme under grant agreement No 821801. More information available at: http://www.efesto-project.eu

8. REFERENCES

[1] Joseph A. Del Corso, F. McNeil Cheatwood, Walter E. Bruce III, Stephen J. Hughes, "Advanced High-Temperature Flexible TPS for Inflatable Aerodynamic Decelerators", 21st AIAA Aerodynamic Decelerator Systems Technology Conference and Seminar, 21st AIAA Aerodynamic Decelerator Systems Technology Conference and Seminar, , AIAA 2011-2510.

[2] J.O. Arnold, R. A. Beck, M. K. McGuire, I. C. Dupzyk, D. K. Prabhu, "Thermal Protection for a Supersonic Inflatable Aerodynamic Decelerator Cover Panel System", AIAA 2011-2570

[3] Stephen J. Hughes, Joanne S. Ware, Joseph A. Del Corso, Rafael A. Lugo, "Deployable Aeroshell Flexible Thermal Protection System Testing", AIAA paper

[4] R. A. Dillman, J. M. Di Nonno, R. J. Bodkin, S. J. Hughes, "Planned Orbital Flight Test of a 6m HIAD". 15th International Planetary Probe Workshop, 2018.

[5] S.J. Hughes., F. McNeil Cheatwood, A.M. Calomino, H.S. Wright, "Hypersonic Inflatable Aerodynamic Decelerator (HIAD)". 21st AIAA Aerodynamic Decelerator Systems Technology Conference and Seminar, 2013.

[6] N. Cheatwood, "Hypersonic Inflatable Aerodynamic Decelerator (HIAD) Technology". NASA's Space Administration Game Changing Technology Industry Day, 2016.

[7] Overend, Samuel J. "European studies to advance development of inflatable and deployable decelerators".

12nd International Planetary Probe Workshop, Koln, Germany. 2015.

[8] Overend et al, "European studies to advance development of inflatable and deployable Hypersonic decelerators". IPPW-14, 2017 The Hague, The Netherlands

[9] G. Guidotti, I. Pontijas Fuentes, F. Trovarelli, I Dietlein, S. Callsen, K. Bergmann, J.L.Verant, R. Gardi, G. Gambacciani, G. Governale, "The EFESTO Project: Advanced European Re-Entry System Based on Inflatable Heat Shield", 2nd FAR congress, Germany, 2022.

[10] Esser, B.; Gülhan, A.; Flow Field Characterisation of DLR´s Arc Heated Facilities L2K and L3K. Proceedings of the 3rd European Symposium on Aerothermodynamics for Space Vehicles, ESTEC, Netherlands, 1998.

[11] Gülhan, A.; Esser, B.; A Study on Heat Flux Measurements in High Enthalpy Flows. 35th AIAA Thermophysics Conference, Paper AIAA 2001-3011, USA, 2001.

[12] Refloch, A., Courbet, B., Murrone, A., Villedieu, P., Laurent, C., Gilbank, P., Troyes, J., Tessé, L., Chaineray, G., Dargaud, J.-B., Quémerais, E., Vuillot, F. CEDRE software. Aerospace Lab Journal, Issue 2, 2011.

[13] Biasi, V. Thermal Modelling of Decomposing Composite Materials Submitted to Fire, PhD thesis. University of Toulouse, 2014.

[14] Park, C. Review of Chemical-Kinetic Problems of Future NASA Missions, I; Earth Entries. Journal of Thermophysics and Heat Transfer. Vol. 7, No. 3, 1993.

[15] Park, C., Howe, J. T., Jaffe, R. L. and Candler, G. V. Review of Chemical-Kinetic Problems of Future NASA Missions, II; Mars Entries. Journal of Thermophysics and Heat Transfer. Vol. 8, No. 1, 1994.

[16] Gülhan, A., Esser, B., Koch, U., Fischer, M., Magens, E. and Hannemann, V. Characterization of High-Enthalpy-Flow Environment for Ablation Material Tests Using Advanced Diagnostics. AIAA Journal. Vol. 56, No. 3, 2018.

[17] Vérant J.-L., Perron N., Balat-Pichelin M., Chazot O., Kolesnikov A., Sakharov V., Gerasimova O., Omaly P. Microscopic and macroscopic analysis for TPS SiC material under Earth and Mars re-entry conditions, Int. J. Aerodynamics, Vol 2, Nos 2/3/4, 2012.

[18] Van Ghele, L. Reulet, P., Vérant, J.-L., Millan, P., Battaglia, J.-L., Aerothermal analysis of the atmospheric reentry of the intermediate experimental vehicle (IXV). International Heat Transfer Conference. Vol. 18. 2018

More information available at: http://www.efesto-project.eu